DRY SLIDING WEAR OF PM Al-10Ti ALLOY①

Wu Nianqiang, Wu Jinming, Lin Shuo, Zhou Jinqi and Li Zhizhang
Department of Materials Science and Engineering, Zhejiang University, Hangzhou 310027, P. R. China

ABSTRACT The wear characteristics of the PM Al-10Ti alloy during dry sliding have been investigated. The wear process can be divided into the running-in stage with high wear rate and the steady-state stage exhibiting mild wear. The transfer layers develop due to deformation, compaction, fracture and adhesion. The oxides consisting of Al_2O_3 and Fe_2O_3 are formed on the worn surface and they reduce wear. Transition from running-in to steady-state wear is caused by strain hardening of subsurface and oxidation of the surface. At the steady-state wear stage, detachment of wear particles is mainly ascribed to delamination of transfer layers.

Key words Al-Ti alloy dry sliding wear delamination

1 INTRODUCTION

During dry sliding of the aluminum alloys and aluminum matrix composites against steels, there exist two distinct wear regimes, i.e., the initial(or running-in) stage with high wear rate and the steady-state stage exhibiting mild wear[1-3]. Dark surface layers are often found during steady-state sliding process of aluminum alloys against the hardened steels[1,4-7]. It has been suggested that the dark layers are mainly composed of aluminum oxides and α-Fe[1-3,7]. But it has also been reported that the dark layers, which result from material transfer across the interface of friction couples, contain only α-Fe and the original phases(such as aluminum and silicon) instead of oxides[4,5]. It has been observed[1,2,5] that the wear debris produced during the steady-state wear consist of relatively large flake-shaped particles(50 μm ~ 1 mm) and small equiaxed particles(< 5 μm). The portion of flake-shaped particles have been raised by increasing applied load. However, only flake-shaped debris have been observed by Pramila Bai[9] in a quite large range of load.

About the steady-state mild wear mechanism of aluminum alloy, there still exists contradiction among conclusions of different researchers. Razavizadeh *et al*[7,11] suggested that oxidative wear occurred via a process of oxidation, deformation and fracture, producing oxide layers on the worn surface. Pramila Bai *et al*[9] proposed that delamination was the only wear mode. While other papers[5,8] have emphasized material transfer between the friction couples, and in this case, oxidation has not been considered as a prevalent mechanism during mild wear.

As described above, the wear characteristics and mechanisms of aluminum alloys are still not adequately understood. It is necessary to study the role of oxidation during sliding wear as well as the correlation between material transfer, delamination and oxidation. In this paper, the wear characteristics of the PM Al-10Ti alloy are investigated.

In addition, an Al-Ti alloy with Al_3Ti as dispersoid has high strength and modulus, low density, good oxidation resistance and strength retention at elevated temperatures. It has potential tribological applications in internal combustion engines or aircrafts[10]. Therefore, the Al-Ti alloy is chosen as a test material.

2 EXPERIMENTAL

The Al-10%Ti alloy powders were atomized with argon gas. Powders in the size range of 63 ~ 90 μm were sealed in an aluminum can in vac-

① Received Nov. 26, 1997; accepted Mar. 30, 1998

uum and compacted into 80 mm diameter round rods at room temperature. The rods were then extruded into bars with rectangular section of 20 mm × 10 mm at 400 ℃. The as-extruded material contained 89.78% Al, 10.10% Ti and 0.12% Fe. The micrograph of the microstructure of the as-extruded alloy shows that the fine Al_3Ti particles with average size of 0.6 μm were dispersed within the α-Al matrix[11]. The hardness of alloy was measured to be 89HV.

Dry sliding wear test was performed using a block-on-ring wear tester of type MLS-23, as described elsewhere[12]. The ring was normalized AISI 1045 steel with hardness of 57 HRC. The block sample and the counter ring were ground and then polished with 1 μm alumina. They were cleaned in acetone prior to wear test. The test was carried out in air with relative humidity of 40% ~ 50% at 25 ℃. The block slide against the steel at relative speed of 1.7 m/s with a load of 40 N. Mass loss was measured with an accuracy of ±0.1 mg.

The worn surfaces, the wear particles and the cross sections(normal to the sliding interface and parallel to the sliding direction) were observed using S-570 scanning electron microscope with EDXA PV-9900 energy dispersive spectrometry. The wear particles were coated with gold prior to examination in SEM. The cross sections were prepared by spark cutting, then embedded in resin, and polished.

The measurement of X-ray photoelectron spectrum(XPS) was performed on the worn surface of the sample with ESCLAB II electron spectrometer with excitation by AlK_α radiation ($h\nu$= 1 481.7 eV). The vacuum in the sample chamber was maintained at 4×10^{-8} Pa. The binding energies were calibrated against the binding energy of the C1*s* electron(284.5 eV).

3 RESULTS

3.1 Wear loss

Fig. 1 shows the cumulative mass loss as function of the sliding distance. The curve in Fig. 1 showed two distinct stages, i.e. an initial (running-in) stage with large wear rate and a steady-state stage at which the cumulative loss nearly increased linearly with the sliding distance, and the wear rate was much smaller than that at the running-in stage.

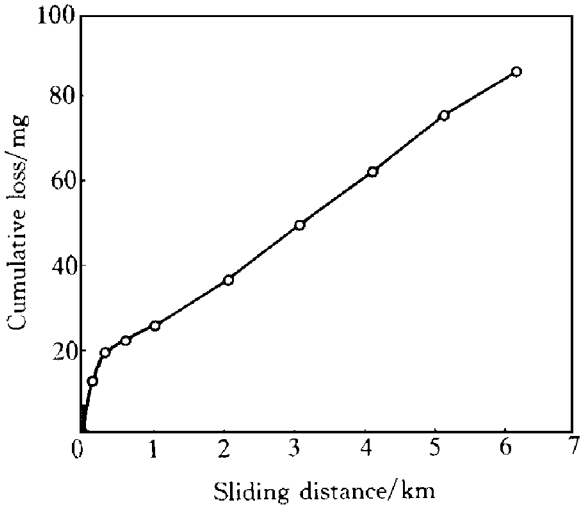

Fig. 1 Cumulative wear loss as function of sliding distance

3.2 Worn surface

Fig. 2 reveals the worn morphologies of the aluminum alloy at the running-in stage. Prows parallel to the sliding direction were seen on the surface(Fig. 2a). A closer look revealed many cracks in each plow, most of them ran in the direction perpendicular to the sliding direction. The wear craters resulting from shear fracture were observed on the worn surface(Fig. 2b).

At the steady-state wear stage, much fewer cracks were observed on the worn surface(Fig. 3). Dark surface layers were formed progressively during wear process. The amount of the layers first increased with the sliding distance and then reached a constant of about 70% of the whole specimen surface. Besides, the wear scars were interspersed in the dark smooth surface (Fig. 3b).

In order to determine the composition of the dark surface layer, X-ray photoelectron spectrum (XPS) shown in Fig. 4 was measured. The analysis of XPS gave 32% Al, 7.2% Fe, 2.7% Ti and 58.2% O (mole fraction). The layer was rich in aluminum and oxygen, and depleted of titanium. In addition, the iron content was much higher than that of the base material. The binding energies of Al2*p*, $Fe2p_{3/2}$ and $Fe2p_{1/2}$ were determined to be 74.8 eV, 710.5 eV and 724.0

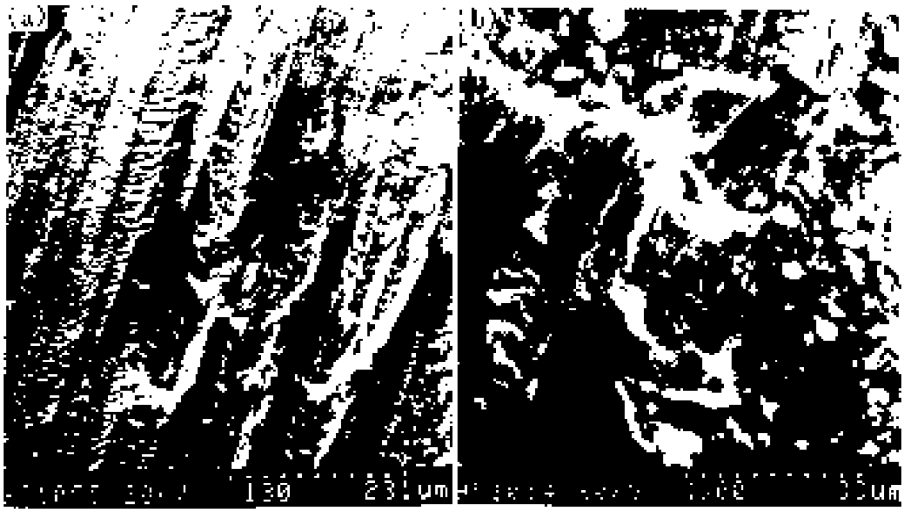

Fig. 2 Worn morphologies of Al-10Ti alloy at running-in stage
(a) —Low magnification; (b) —High magnification

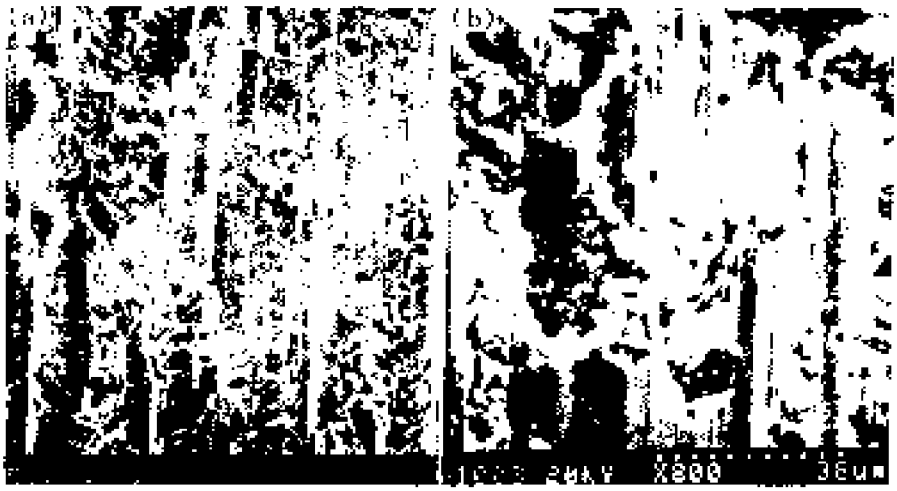

Fig. 3 Worn surface of Al-10Ti alloy at steady-state stage
(a) —Low magnification; (b) —High magnification

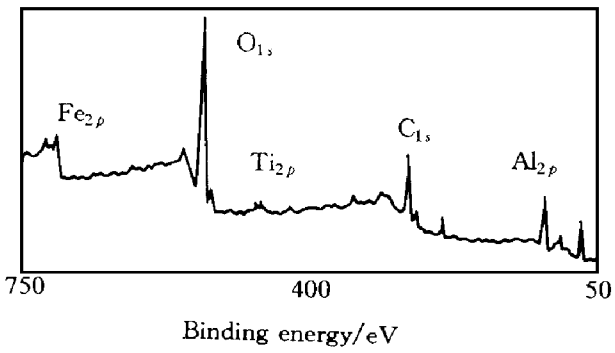

Fig. 4 XPS spectrum of dark surface layer

eV, respectively. The spectrum of O_{1s} was resolved into two peaks, i. e., one with higher binding energy of 531. 4 eV, the other with 529. 9eV. Therefore, according to the handbook of XPS[14], there should exist Al_2O_3 and Fe_2O_3 in the dark surface layer. This result indicated that iron was transferred from the counterface to the surface of the aluminum alloy and the oxides are formed there.

An examination of the steel ring showed that the aluminum alloy had transferred to the counterface, resulting in the deposit layers on the counterface (Fig. 5). This indicates that transfer-back-transfer of materials between the friction couples took place.

3.3 Cross section

Fig. 6 also shows the back-transferred mate-

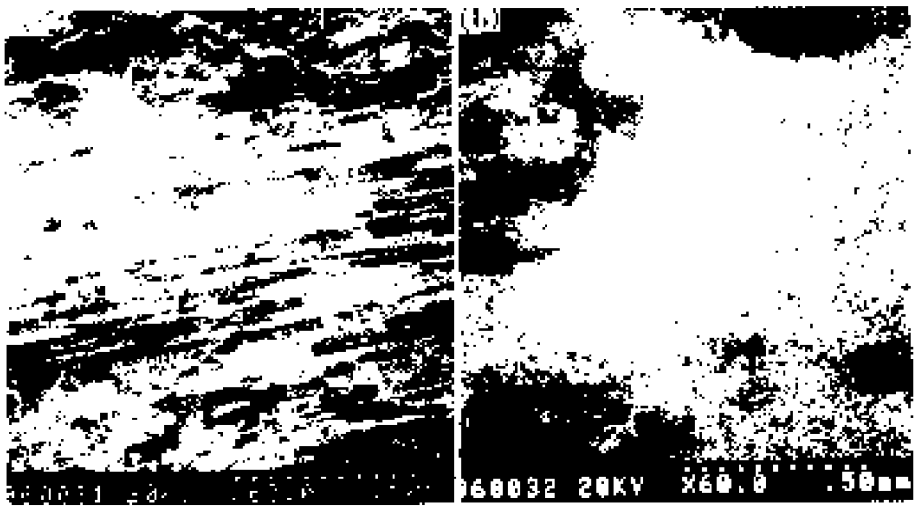

Fig. 5 Al alloy deposited on counter steel
(a) —Worn morphology; (b) —AlK_α dot map

Fig. 6 SEM micrograph of cross section of worn Al-10Ti alloy

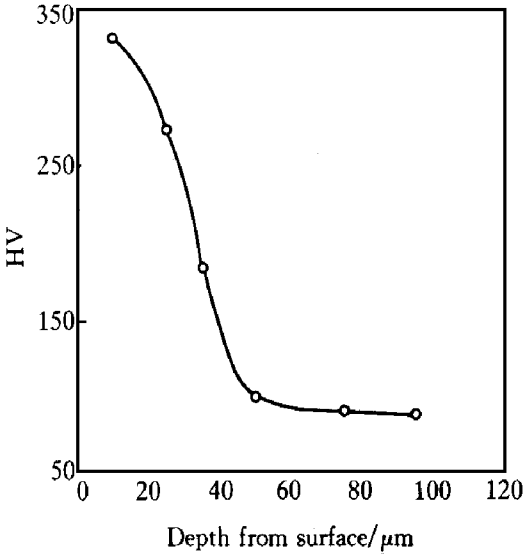

Fig. 7 Work hardening of transfer layer

rial on the surface of block specimen. The dark surface layers had lamella structure. Cracks parallel to the worn surface were present not only at the interface of transfer and base material but also within the transfer layers(Fig. 6).

The hardness of transfer layer was higher than that of base material(Fig. 7). In addition, Fig. 7 shows a decrease in hardness from the outermost layer into subsurface, implying a varying work-hardening dependence on the depth from surface. It was evident that the spherical Al_3Ti particles were dispersed in the Al matrix. However, the numbers of Al_3Ti particles within subsurface were fewer than those in base material.

3.4 Wear debris

Fig. 8a shows the morphologies of the wear debris produced at the running-in stage. The large irregular flake-shaped particles were dominantly present. Such particles with the size of 40 ~ 400 μm were typical of ductile shear fracture. The wear particles generated at the steady-state stage are shown in Fig. 8b. Most of the particles (8~ 40 μm) were flake-shaped and much smaller than those produced at the running-in stage. In addition, the small equiaxed particles(< 5 μm) were present. Our previous X-ray diffraction[13] has shown that trace of α-Al_2O_3 was detected in the wear particles generated at the steady-state stage. This indicates that oxidation may occur in the transfer layers.

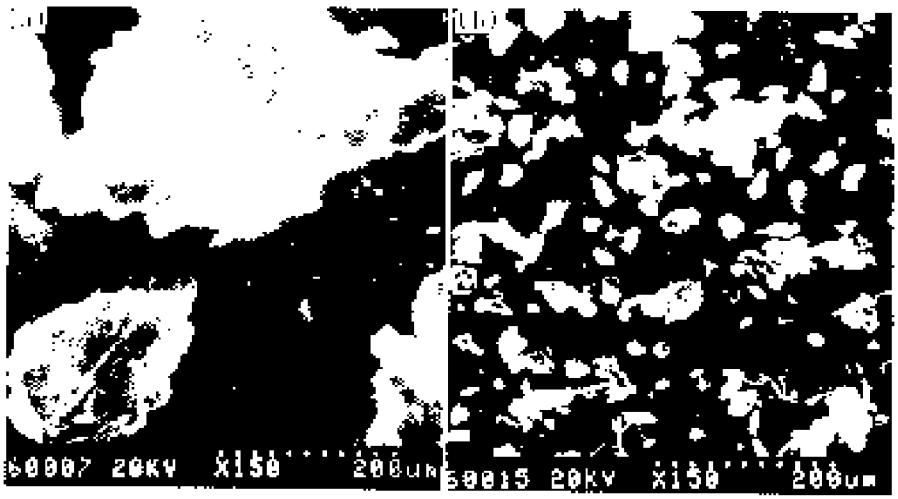

Fig. 8 Wear debris produced at running-in stage(a) and generated at steady-state stage(b)

4 DISCUSSION

As described above, the Al-10Ti alloy exhibits running-in and steady-state wear during sliding process. This is in agreement with the wear behaviors of some other aluminum-based materials, such as Al-Si alloys[1], 2024 alloy[2] and aluminum matrix composites[3]. At the initial wear stage, the metallic asperities of aluminum alloy directly contact with the steel counterface. The surface suffers shear fracture and the fracture layers are rolled into large flake-shaped particles between the friction couples. Since the aluminum alloy has a relatively low hardness and good ductility, the alloy shows poor wear resistance.

As wear progresses, the higher asperities are deformed and then cover the lower ones if they are not detached from the surface. The lower asperities are also deformed and covered the others. As a result, the shear plates are established(as shown in Fig. 2). If the asperities are fractured, part of them will become debris, and the rest will be adherent to the counterface (see Fig. 5). The transferred material on the counterface, which is mixed with iron, may again be transferred to the surface of the block later. Therefore, the surface layers of the block specimens consist of the transferred materials and is thus also called the transfer layers. In this study, the transfer layers appear as the dark smooth region interspersed with the wear scars (Fig. 3), which contains Fe(as confirmed in Fig. 4). During transition from the running-in stage to the steady-state stage, more and more surface of the specimen is covered with the transfer layer, until the dynamic steady-state stage has been reached. The surface portion covered with the transfer layers stays a constant(about 70% of the whole surface): i) the materials are removed from the worn surface, ii) the locally exposed base material allows formation of supplementary transfer layers, consequently the transfer layers are replenished. Thus the fundamental aspect of the steady-state wear is the cyclic transfer-back-transfer of materials, accompanied by detachment of material from the worn surface.

The test shows that Al_2O_3 and Fe_2O_3 are present in the transfer layers. These oxides on the worn surface have significant influence on the wear process. First, the metal oxides have lower coefficient of friction as compared to the alloys[15]. They provide in-situ lubricants, which can lead to decrease in the crack nucleation depth and crack growth rate. Second, the oxides reduce adhesion of aluminum alloy to counter steel. However, they also decrease adhesion of the transfer layers to each other as well as adhesion of the transfer layers to the base material. In addition, if the oxides are embedded in the transfer layers during the transfer process, they may provide sites for crack nucleation. In the present study, we believe that the positive

effects of oxides are dominant during sliding wear. Besides the effects of oxides, work-hardening of the surface layers(Fig. 7) can also result in a reduction of wear rate. Transition from running-in to steady-state wear is thus probably controlled by both oxidation of surface and strain hardening of the regions adjacent to the contact surface.

The deformation and microcracks in the subsurface(Fig. 6) as well as the flake-shaped wear debris(Fig. 8b) indicate that delamination is the dominant wear mechanism at the steady-state wear stage[16, 17]. In the ductile materials, nucleation and propagation of wear crack in sliding system can be regarded as a damage accumulation process[18]. As sliding proceeds, severe plastic deformation was localized within the transfer layers adjacent to the worn surface, accompanied by work-hardening(Fig. 7). As proposed by Alpas *et al*[19], the voids may nucleate in the intersection of shear bands(in the regions where the material's work-hardening capacity is exhausted) or at the oxides inclusions which are embedded in the transfer layers. Nucleation and growth of voids lead to formation of microcracks (see Fig. 6). If the shear strain at the regions under the contact surface exceeds a critical criterion, the microcracks will propagate in the direction parallel to the contact surface, leading to delamination of the transfer layers. As a result, materials are detached in the form of flake-shaped particles(Fig. 8b).

5 CONCLUSIONS

(1) The Al-10Ti alloy exhibits running-in and steady-state wear stages during sliding against steel.

(2) The transfer layers are established during sliding. Severe plastic deformation and strain hardening are localized within the transfer layers. And the oxides consisting of Al_2O_3 and Fe_2O_3 have formed on the worn surface and can reduce wear.

(3) Transition from running-in to steady-state wear is controlled by strain hardening of subsurface and oxidation of surface.

(4) At the steady-state wear stage, delamination is the dominant wear mechanism. As a result, materials are detached from the transfer layers, leading to the formation of small flake-shaped wear particles.

REFERENCES

1 Davis F A and Eyre T S. Tribology Inter, 1994, 27(3): 171.
2 Yoshiro T, Hidetomo Y and Tomoni H. Wear, 1995, 181– 183: 594.
3 Wang A and Rack H J. Wear, 1991, 147: 355.
4 Antoniou R A, Brown L J and Cashion J D. Acta Metall Mater, 1994, 42(10): 3545.
5 Antoniou R and Borland Douglous W. Mater Sci Eng, 1987, 93: 57.
6 Clark J and Sarkar A D. Wear, 1982, 82: 179.
7 Razavizadeh K and Eyre T S. Wear, 1982, 179: 325.
8 Rigney D A, Chen L H and Naylor M G S. Wear, 1984, 100: 195.
9 Pramila Bai B N and Biswas S K. ASLE Trans, 1986, 29(1): 116.
10 Wu N Q, Wang G-X and Li Z Z. Mater Sci Eng Sinica, (in Chinese), 1994, 12(4): 39.
11 Wu N Q, Wang G-X, Li Z Z, Wu J M and Chen J W. Wear, 1997, 203– 204: 155.
12 Wu N Q, Wang G-X and Li Z Z. In: Proc Third Seminar of CAIME, (in Chinese), Leshan City, China, Oct. 1995.
13 Wu N Q, Wang G-X and Li Z Z. Trans Nonferrous Met Soc China, 1997, 7(1): 82.
14 Wagner C D, Riggs W M, Davis L E, Moulder J F and Muilenberg J E. Handbook of X-ray Photoelectron Spectra. Perkin-Elmer Corporation Physical Electronics Division, 1979.
15 Alpas A T and Zhang J. Metall Trans A, 1994, 25A: 969.
16 Suh N P. Wear, 1973, 25: 111.
17 Suh N P. Wear, 1977, 44: 1.
18 Lerroy G, Embury J D, Edwards G and Ashby M F. Acta Metall, 1981, 29: 1509.
19 Alpas A T and Embury J D. Wear, 1991, 146: 285.

(Edited by Peng Chaoqun)